Electrosynthesis of a Duplex Coating Consisting of a Cerium-Based Layer and a Polypyrrole Film for the Corrosion Protection of AISI 304 Stainless Steel

A.P. Loperena, I.L. Lehr* and S.B. Saidman

Instituto de Ingeniería Electroquímica y Corrosión (INIEC), Departamento de Ingeniería Química, Universidad Nacional del Sur (UNS), CONICET, Bahía Blanca, Argentina

Abstract: Duplex coating consisting of an inner cerium-based layer and polypyrrole (PPy) film topcoat was electrodeposited onto AISI 304 stainless steel. The cerium-based coating was electrodeposited in solutions containing cerium nitrate at 50 ºC. The polymeric outer layer was electropolymerized in the presence of sodium bis(2-ethylhexyl) sulfosuccinate (AOT). The electrosynthesis was done under potentiostat conditions. The coatings were characterized by scanning electron microscopy (SEM) and energy dispersive x-ray spectrometry (EDX). The morphology of the double-layered cerium polypyrrole film shows a granular structure with the presence of agglomerates of small grains.

The anticorrosive performance of the coatings was evaluated in sodium chloride solution by linear polarization, open circuit measurements, and electrochemical impedance spectroscopy (EIS). Single films, cerium layer and PPy coating, and the duplex film all reduce the corrosion rate of AISI 304 stainless steel in NaCl solution. The duplex coating presents an improved corrosion resistance concerning the single films. The combination of the characteristics of the single layers is responsible for the superior corrosion protection efficiency of the double-layered cerium polypyrrole coating.

Keywords: Cerium-based film, Polypyrrole, Duplex coatings, AOT, Anticorrosive properties, AISI 304 SS.

1. INTRODUCTION

Type 304 stainless steel is widely used for a variety of household and industrial purposes due to its mechanical properties. Nevertheless, this material suffers pitting corrosion in aqueous solutions, which limits its potential applications [1, 2]. Consequently, much effort has been expended in attempting to understand and overcome pitting corrosion. One alternative to avoid this type of degradation is the use of protective coatings. Different electrochemical treatments were carried out to generate anticorrosive films. Between them, conversion treatments are known for their low cost and simplicity of operation [3, 4]. Conversion coatings provide corrosion protection due they act as a barrier between the substrate and the corrosive environment and/or through the presence of corrosion inhibitors in the film [5]. Cerium based conversion coating is one of the most promising environment-friendly chemical treatments to modify the steel surface properties since cerium ions are considered good corrosion inhibitors [6]. However, it has been reported that the improvement achieved with this type of coatings is not significant because its non-compact morphology and cracked and porous structure that facilitates the electrolyte diffusion to the substrate [7]. Golden *et al.* have been informed of an enhancement of the anticorrosive properties of stainless steel (type 430) by anodic deposition of cerium oxide films [8].

On the other hand, conducting polymers have been widely studied to improve the corrosion resistance of metallic substrates. Among these polymers, polypyrrole (PPy) has been extensively investigated due to its physicochemical stability, high conductivity, easy processability and relatively low cost [9]. Several studies have reported that the electrosynthesis of polypyrrole (PPy) films on pure iron [10, 11], mild steel [12-14] and stainless steel [15-18] can effectively inhibit the corrosion of these materials. It has been proposed that PPy coatings protect metallic substrates through a mixed mechanism of isolation and charge transfer [18]. Moreover, it has been demonstrated that the use of sodium bis(2-ethylhexyl) sulfosuccinate (AOT) in the chemical synthesis of PPy significantly increases the conductivity of the polymer due to the incorporation of the anionic part of the surfactant into the PPy chains [19]. In previous works, we showed that AOT plays a dual role as a dopant and as a surfactant in the electrodeposition process of PPy [20-22]. Motheo *et al*. have been reported a good anticorrosive performance of cerium conversion and polyaniline duplex coatings formed on AA6063 aluminium alloy [23]. The general corrosion protection mechanism has been attributed to the presence of cerium-based film acting as a barrier and the anodic protection provided by the conducting polymer.

*Address correspondence to this author at the Instituto de Ingeniería Electroquímica y Corrosión (INIEC), Departamento de Ingeniería Química-Universidad Nacional del Sur- Av. Alem 1253, 8000- Bahía Blanca – República Argentina; Tel/Fax: 54 291 4595182; E-mail: ilehr@uns.edu.ar

E-ISSN: 2410-4701/21

In this study, the formation of a duplex coating onto AISI 304 stainless steel is presented. The objective was to combine the properties of the cerium-based layer with those of the PPy film. In this regard, the inner layer was obtained in a solution containing cerium nitrate and the outer film was PPy doped with AOT. The influence of different parameters on the anticorrosive performance of the duplex coating was analyzed. The characterization of the films was done using electrochemical techniques and SEM/EDX. For comparative purposes, the anticorrosive behavior was also checked for the single films and the uncoated AISI 304 stainless steel.

2. EXPERIMENTAL

AISI 304 stainless steel (AISI 304 SS) rod samples were used as working electrodes. The rods with an exposed area of 0.070 cm^2 were inserted in a Teflon holder. Before the coating formation, the exposed surfaces were ground from 600 to 1200 grit SiC paper. Subsequently, the electrodes were cleaned with acetone and rinsed with triply distilled water. After this pretreatment, the samples were immediately introduced to the electrochemical cell.

A saturated Ag/AgCl and a platinum plate were employed as the reference and counter electrodes, respectively. Electrochemical tests were performed using a potentiostat–galvanostat Autolab PGSTAT 128N and PAR Model 273A. The impedance measurements were done in the frequency range of 10 Mhz to 100 kHz and the perturbation signal amplitude was 10 mV. Surface morphologies and element compositions of the films were studied by a dual-stage ISI DS 130 SEM and an EDAX 9600 quantitative energy dispersive X-ray analyser, respectively.

Before the electropolymerization, the AZ91D samples were immersed in a cerium nitrate hexahydrate ($Ce(NO_3)_3.6H_2O$) solution at 50ºC for 30 min. The polymer was electrodeposited at 0.90 V during 1800 s in a solution containing 0.05 M AOT and 0.50 M Py, pH 6. Pyrrole (Sigma – Aldrich) was freshly distilled under reduced pressure before use.

A Mecmesin basic force gauge (BFG 50N) and a Scotch® Magic™ double-coated Tape 810 (3M) were used to measure the force necessary to peel off the film.

The potentiodynamic method, the variation of the open circuit potential (OCP) as a function of time and electrochemical impedance spectroscopy (EIS) were employed to evaluate the corrosion performance of samples in aerated 0.50 M NaCl solution. Before the ac measurements, the electrodes were allowed to equilibrate at the fixed voltage. Furthermore, the EIS data were analyzed and modelled into equivalent electrical circuits (EEC) with Z-View software.

The Tafel measurements were made by polarizing from cathodic to anodic potentials concerning the OCP at 0.001 Vs^{-1} in aerated 0.50 M NaCl solution. Tafel extrapolation method allows estimating the corrosion parameters. In the case of reactions controlled by charge transfer, the corrosion current density (i_{corr}) at the corrosion potential (E_{corr}) can be obtained from the extrapolation of anodic and/or cathodic lines. Each experiment was carried out after 1 h of immersion in the solution to guarantee that steady-state E_{corr} was reached.

To ensure reproducibility and minimize experimental error, all experiments were independently repeated (duplicates or triplicates).

3. RESULTS AND DISCUSSION

3.1. Cerium Deposition

In order to establish the best conditions for cerium-based coating formation, deposition parameters such as the applied potential, immersion time and bath temperature were analyzed. In this way, potentiodynamic polarizations in 0.50 M NaCl of the electrodes treated in different cerium-based baths were carried out.

Adherent greyish-white films were obtained on AISI 304 SS after immersion in a 50 mM $Ce(NO_3)_3$ solution at 50 ºC after polarization in the potential range between - 0.20 V and - 0.60 V during 30 min. Polarization measurements in 0.50 M NaCl solution for cerium coatings synthesized at different potentials are presented in Figure **1**. For comparison, the curve obtained for the untreated substrate is also included (Figure **1**, curve a). As it could be seen from the curve, the active dissolution of the alloy starts at approximately 0.20 V. All the formed films modify the potential value of the beginning of the dissolution. It is noticeable that the Ce layer formed at - 0.20 V shows the best anticorrosive performance (Figure **1**, curve d), leading to a shift in the potential value to around 1.50 V. The corresponding curve initially exhibits low current densities, indicating that the corrosion reaction of AISI 304 SS is retarded by the presence of the coating. Considering this result, the cerium-based coating selected for further experiments will be

electrodeposited onto AISI 304 SS at - 0.20 V under the mentioned conditions. The transient obtained for the formation is shown in Figure **2**, curve a. This single layer will be called Ce film.

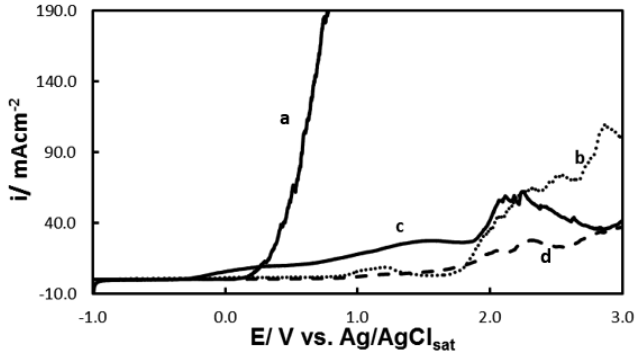

Figure 1: Polarization behavior in 0.50 M NaCl at 0.001 Vs^{-1} of AISI 304 SS uncoated (**a**), and coated with cerium-based films formed in 50 mM $Ce(NO_3)_3$ pH 4.7 during 30 min at: - 0.20 V (**b**), - 0.40 V (**c**) and - 0.60 V (**d**).

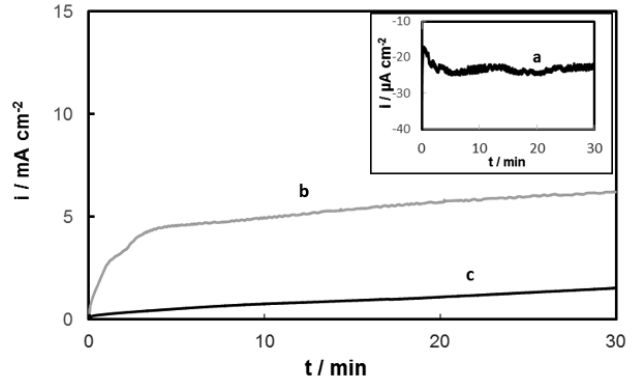

Figure 2: Potentiostatic transients obtained for AISI 304 SS during the formation of: Ce film (**a**), PPy film (**b**) and Ce/PPy duplex coating (**c**).

Normand *et al*. have reported that cerium-based electrochemical treatments enhance the corrosion resistance of stainless steel due to a chromium enrichment in the passive layer [24]. When the substrate is immersed in the electrolyte solution the chromium present in the alloy reacts with the dissolved oxygen. In addition, it has been informed that an increment in the pH at the electrode surface was caused by electrochemical reactions such as the reduction of water, dissolved oxygen or nitrates, leading to the formation of cerium hydroxide due to the hydrolysis of Ce^{3+} [25]. Thus, in aerated solutions, $Ce(OH)_3$ is oxidized to $Ce(OH)_4$ which reacted with electrogenerated OH^- ions to form a precipitate of CeO_2 [26]. In the same way, an oxidation mechanism has been proposed for the Cr_2O_3 formation [6]. As a result, the coating is composed of oxides/hydroxides of cerium and chromium.

3.2. Electrosynthesis of PPy Films

In previous works, we reported the electrosynthesis of uniform and adherent polypyrrole (PPy) films on SAE 4140 steel obtained in solutions containing 0.05 M AOT [27]. Uniform and adherent PPy films were obtained on AISI 304 SS at 0.90 V for 30 min in a solution containing 0.05 M AOT and 0.50 M Py, pH 6. Figure **2**, curve b shows the potentiostatic transients obtained for the synthesis of PPy films on AISI 304 SS. Initially, the magnitude of the current decreases, which is associated with oxide growth and, after this stage, the formation of the polymer starts. At the end of the potenciostatic procedure, the substrate surface was completely covered with a black PPy film.

3.3. Electrodeposition of the Duplex Coating

The adherent duplex coating was formed by a potentiostatic method. As mentioned previously, the inner layer was the Ce film. The coated electrode was rinsed with tridistilled water before being immersed in the electrochemical cell for the electrodeposition of the outer layer. This polymeric film was electro synthesized at 0.90 V for 30 min in a solution containing 0.05 M AOT and 0.50 M Py at pH 6 (Figure **2**, curve c). The charge consumed during the electrosynthesis of the outer layer is approximately 30 percent of the charge involved in the electroformation of the PPy coating doped with AOT onto the uncoated steel, which is obviously due to the presence of the inner film. For practical purposes, the duplex coating will be called Ce/PPy coating.

3.3.1. Coatings Characterization

The SEM images of the single films and the duplex coating are shown in Figure **3**. Ce film is constituted by worm-like deposits with dimensions in the order of 2 μm similary to the morphology reported by Vakili at el. (Figure **3A**) [28]. Figure **3B** shows the typical granular structure of PPy film. Ce/PPy duplex coating also shows the granular structure with the presence of agglomerates of smaller grains (Figure **3C**).

EDX analysis of all obtained coatings is presented in Figure **4**. EDX spectrum confirms the presence of cerium in the Ce film (Figure **4A**). As it was mentioned, cerium-based films are formed from the precipitation of oxides, due to an increase in local pH at the interface substrate/solution. The presence of sulfur in the EDX spectrum obtained for the PPy film indicates that AOT was incorporated into the polymer matrix (Figure **4B**). It was demonstrated that the AOT surfactant is incorporated into the PPy chain similarly as the dopant

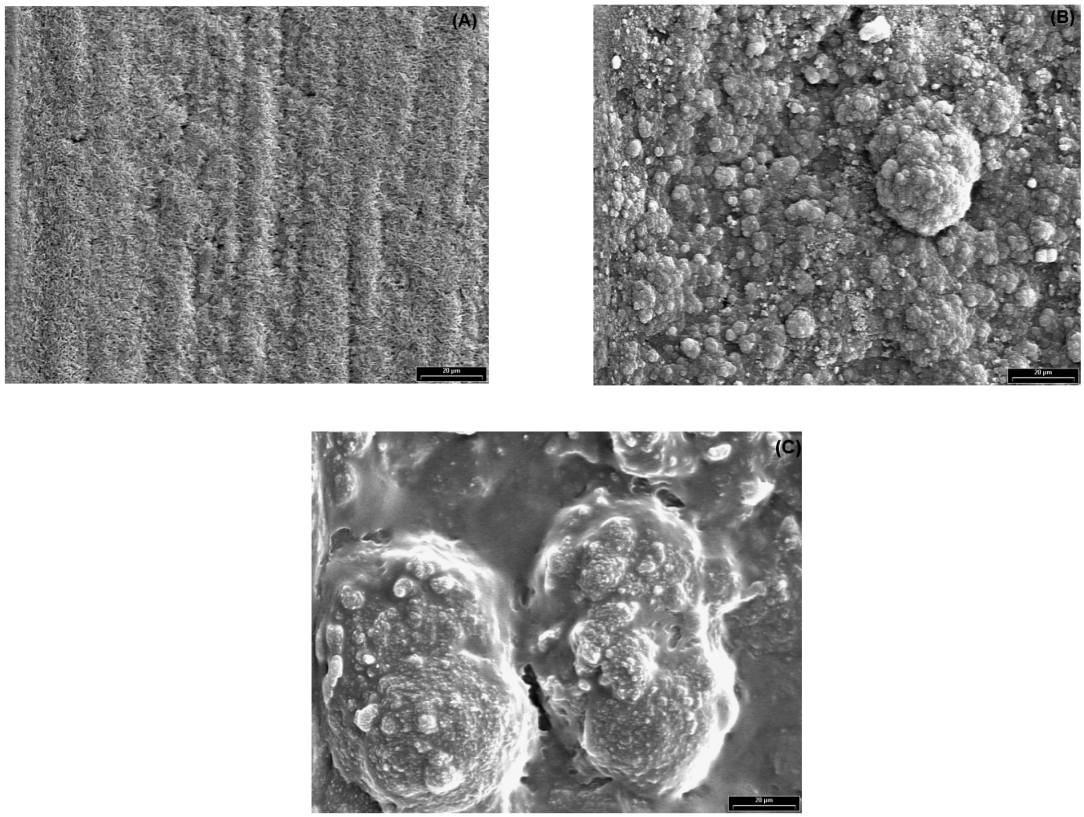

Figure 3: SEM micrographs of AISI 304 SS coated with: Ce film (**A**), PPy film (**B**) and Ce/PPy coating (**C**). Magnification 1000x.

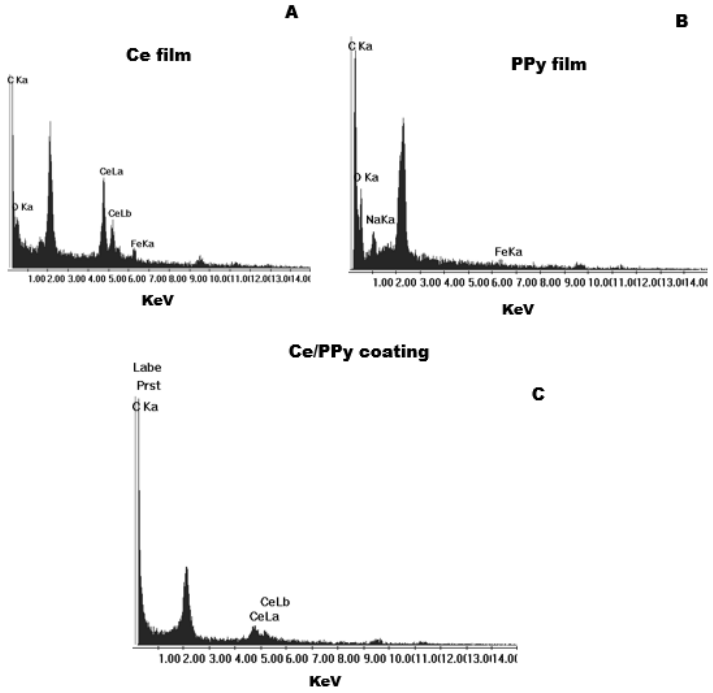

Figure 4: EDX spectra of AISI 304 SS coated with: Ce film (**A**), PPy film (**B**) and Ce/PPy coating (**C**).

anion does [19]. EDX spectrum of the duplex coating (Figure **4C**) confirms that both AOT and Ce are present in the bilayer.

The chemical composition of the coating was analyzed by XPS. The overall XPS survey and high resolution deconvoluted C 1s, N 1s, O 1s and Ce 3d

was presented in Figure **5A**. C, N, O, and Ce were detected as the major elements. As shown in Figure **5B** the C 1s spectrum can be decomposed into five peaks: 284,4 eV for β carbons of the pyrrolic chains and adventitious C; 285.1 eV for α carbons of the pyrrole chains and C-C and C-H of AOT; 286.3 eV for C=N of the pyrrole rings and the bipolarons ($-C=N^+$) and C-O and $C-SO_3^-$ of AOT; 287 eV for the bipolarons ($-C=N^+$) and C=O; 289.5 eV for O-C=0 of AOT [29-32]. The high-resolution N 1s spectrum can be fitted using two components corresponding to -NH- (399.5 eV) and $-N^+-$ species (400.9 eV) (Figure **5C**) [34-36].

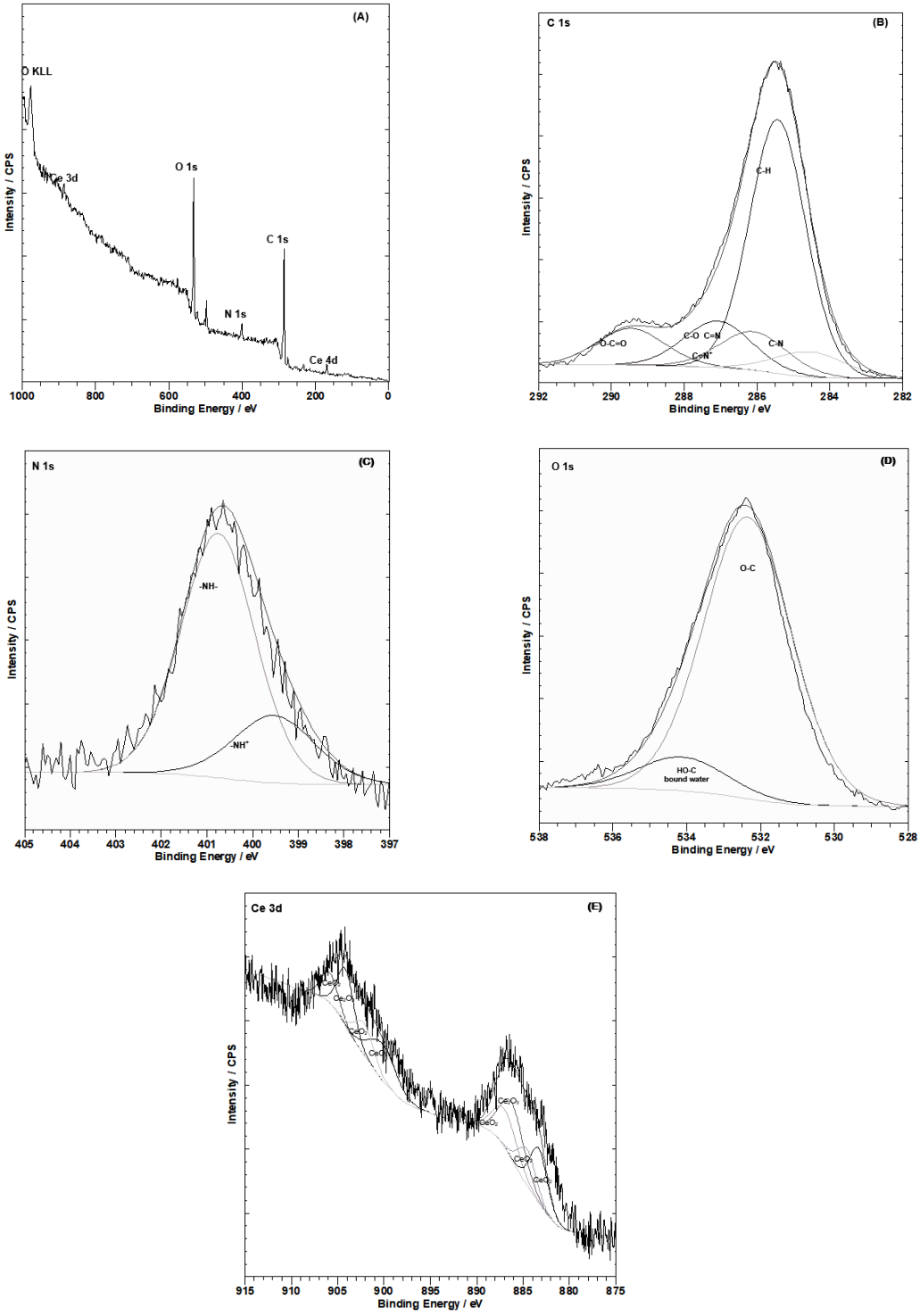

Figure 5: (**A**) XPS survey spectrum of Ce/PPy coating. XPS intensities of: (**B**) C 1s, (**C**) N 1s, (**D**) O 1s and (**E**) Ce 3d.

The O 1s signal was deconvoluted into two peaks at binding energies of 532.6 eV, and 533.6 eV related to O=C, HO–C and bound water, respectively (Figure **5D**) [35, 37]. In Figure **5E**, the high-resolution Ce 3d spectrum shows the presence of two types of cerium oxides, CeO_2 and Ce_2O_3. In this case, the deconvoluted peaks of Ce 3d at about 905.1 eV, 902.2 eV, 889.5, 887.2 eV, 883.7 eV and 882.5 eV are attributed to the Ce^{4+} and the peaks at 903 eV and 886.2 eV correspond to Ce^{3+} [38, 39]. The Fe 2p signal corresponding to the substrate is undetectable probably associated with the high thickness of PPy film.

Mechanical polishing was required to remove all the coatings. The adhesion force, so-called pull-off force, of the different coatings, is informed in Table **1**. The Ce and PPy films present values of 19.30 and 26.40 N respectively. Whereas the duplex coating needed 37.10 N to be removed. Even though the necessary forces to peel off the films are all of the same order of magnitude, the dual-layer (Ce-PPy coating) is the most adherent. Moreover, the presence of Ce film improves the adherence of the PPy coating on the AISI 304 SS.

Table 1: Adherence Force Obtained for Different Coatings Coated AISI 304 SS after Peel-off Testing

Sample	Adherence Force (N) ± 0.10
Ce layer	19.30
PPy film	26.40
Ce/PPy coating	37.10

3.3.2. Anticorrosive Properties of the Duplex Coating

The variation of the open circuit potential (OCP) as a function of time roughly describe the grade of corrosion protection achieved with the generated films. The OCP was monitored in 0.50 M NaCl for all the obtained coatings and the curves are presented in Figure **6**. The pitting potential of the uncoated electrode is - 0.276 V vs. $Ag/AgCl_{sat}$ (Figure **6**, curve a). There is a clear ennoblement in the OCP for the coated electrodes (Figure **6**, curves b, c and d). The initial OCP value for Ce film was - 0.050 V (Figure **6**, curve b). Then, the OCP decreases until around - 0.105 V where it remains for approximately two days. After 3 days of immersion, the OCP value is approximate - 0.180 V, reaching the corrosion potential of the uncoated substrate. The behavior of single PPy films is presented in Figure **6**, curve c. In this case, the initially measured potential is 0.040 V but it drops relatively fast and the corrosion potential of the uncoated AISI 304 SS is reached after five days of immersion. The protection time for the two single coatings is shorter compared to that of the double-layered Ce/PPy coating (Figure **6**, curve d). The curve for the duplex film starts at 0.200 V and after ten days, the OCP value is approximate - 0.038 V, which is still more positive than that for the uncoated alloy. These results suggest that the Ce/PPy coating is a very efficient barrier for protecting the steel against corrosion.

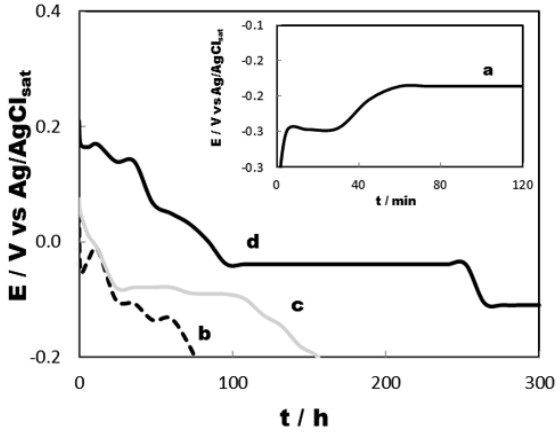

Figure 6: Time dependence of the OCP in 0.50 M NaCl solution of the bare AISI 304 SS (**a**) and those of the alloy covered with: Ce film (**b**), PPy film (**c**) and Ce/PPy coating (**d**).

Table 2: Elemental Analysis Corresponding to a 0.50 M NaCl Solution after a Sample was Immersed: Uncoated AISI 304 SS and Coated with Ce Film after 3 Days of Immersion; PPy Film, after 5 Days of Immersion and Ce/PPy Duplex Coating after 10 Days of Immersion

Sample	Immersion Time / days	Fe (mg/L) ± 0.03
Uncoated AISI 304 steel	3	3.20
Ce film	3	2.60
PPy film	5	2.10
Ce/PPy coating	10	1.44

To verify the enhancement in the corrosion protection of the steel, the Fe quantity released under OCP conditions in 0.50 M NaCl solution during different immersion times was compared (Table **2**). In the case of the bare substrate, the time of immersion was shorter (3 days) with a result of 3.20 mg/L. The quantity of Fe released was low when the substrate was coated, being 2.60 and 2.10 mg/L for the Ce and PPy simple films respectively. When the substrate was coated with the duplex coating, the Fe quantity released after 10

Table 3: Corrosion Parameters Calculated from Tafel Polarization Plots for AISI 304 SS, Ce film, PPy Film and Ce/PPy Coating

Sample	E_{corr} / V vs. Ag/AgCl$_{sat}$	i_{corr} μA/cm^2	B_c / mV dec^{-1}	B_a / mV dec^{-1}
Uncoated AISI 304 steel	- 0.27 ± 0.02	1.65 ± 0.05	- 108.0	206.1
Ce film	- 0.52 ± 0.03	0.55 ± 0.03	- 336.4	101.0
PPy film	- 0.49 ± 0.03	0.13 ± 0.02	- 206.0	86.0
Ce/PPy coating	- 0.79 ± 0.05	0.06 ± 0.01	- 148.2	283.5

days was 1.44 mg/L, corroborating a better performance even after a long exposure time. The formation of PPy layer on top of the Ce film seems to block the pores of the inner layer which prevents chloride ingress.

Figure **7** shows the Tafel plots of the AISI 304 SS electrode covered by single films (Ce film and PPy film) and duplex coating (Ce/PPy coating). For comparison, the curve obtained for uncoated steel is presented (Figure **7**, curve a). Estimation of the corrosion parameters (E_{corr}, cathodic (B_c) and anodic (B_a) Tafel slopes and corrosion current (i_{corr})) are reported in Table **3** for all studied coatings. The i_{corr} value measured for the uncoated AISI 304 SS was 1.65 μA cm^{-2}, whereas the covered substrate show values of 0.55, 0.13 and 0.06 μA cm^{-2} for the Ce, PPy and Ce/PPy coatings respectively. All the coated samples present values significantly lower than that of the bare steel. The duplex coating presents the lowest corrosion rate (Figure **7**, curve d).

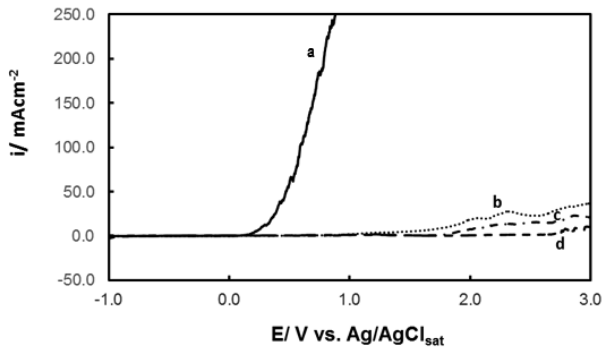

Figure 7: Tafel curves obtained in 0.50 M NaCl solution of the bare AISI 304 SS (**a**) and those of the alloy covered with: Ce film (**b**), PPy film (**c**) and Ce/PPy coating (**d**).

Polarization curves for the uncoated steel, single layers and duplex coating in 0.50 M NaCl solution are presented in Figure **8**. For the single films, high current densities with small oscillations were registered (Figure **8**, curve b and c). In both cases, the yellow colouration of the NaCl solution denoted iron dissolution at the end of the procedure. On the other hand, a significant improvement in the corrosion resistance is obtained when the substrate is coated by the duplex coating (Figure **8**, curve d). The corresponding curve initially exhibits low current, indicating that the corrosion reaction of the substrate is retarded. At the end of the potential scan, the coating deterioration is not visible to the naked eyes. Moreover, the chloride solution did not present the typical yellow colouration indicative of iron dissolution. Thus, the Ce/PPy duplex coating is the most effective in hindering the access of pitting-causing aggressive anions to the surface of steel compared to single films.

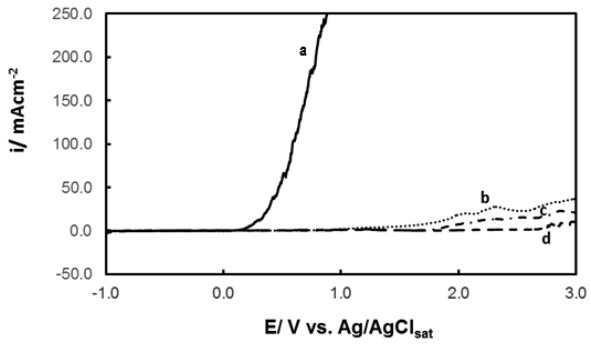

Figure 8: Polarization behavior in 0.50 M NaCl at 0.001 Vs^{-1} of: the bare AISI 304 SS (**a**) and those of the alloy covered with: Ce film (**b**), PPy film (**c**) and Ce/PPy coating (**d**)

To analyze the anticorrosive behavior of the coatings at different immersion times in aereated 0.5 M NaCl solution, EIS measurements were carried out. Figure **9** shows the Nyquist diagrams for the electrode covered with the singles and duplex coatings. For comparison, the impedance spectrum of the uncoated AISI 304 SS is also presented (Figure **9**, curve a). At the beginning of immersion, the impedance spectrum for all coatings shows two incomplete semicircles (Figure **9**, curve b, c and d). The semicircle at high

frequencies is attributed to the charge transfer resistance against the substrate dissolution in parallel with electrical double layer capacitance [28,29]. At lower frequencies, the incomplete semicircle is associated with the presence of the inner barrier layer of corrosion products [30,31]. A remarkable difference in the Nyquist plot of the duplex coating compared to the spectra obtained for the single films is the increase in the total impedance. It is known that a high total impedance is associated with the best corrosion resistance of the coatings. This result also corroborated that the Ce/PPy duplex coating improves the corrosion performance significantly.

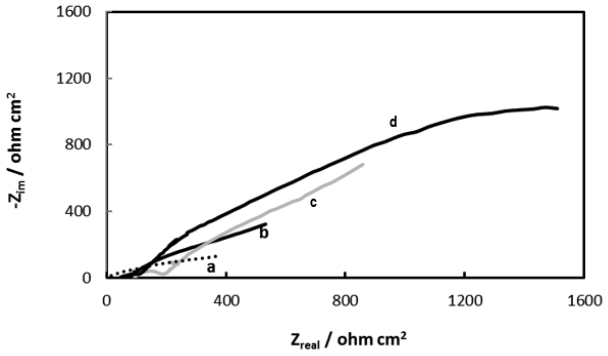

Figure 9: Nyquist plots of the impedance spectra for the coatings at the open circuit potential in 0.50 M NaCl after 5 min of immersion for the bare AISI 304 SS (**a**) and those of the alloy covered with: Ce film (**b**), PPy film (**c**) and Ce/PPy coating (**d**).

Figure **10** shows the Nyquist plots obtained for the Ce/PPy coating at different immersion times in 0.50 M NaCl solution. As can be observed, the total impedance increases with the immersion time. However, it is interesting to note that after 7 days of immersion a diffusional contribution is visible in the impedance spectra (Figure **10**, curves b and c). It has been reported that the linear part in the low-frequency region is associated with a corrosion reaction controlled by mass transfer limitations [32]. Thus, the duplex coating behaves as a blocked electrode. This result corroborates that the Ce/PPy duplex coating can effectively improve the corrosion resistance of the AISI 304 SS in NaCl solution. In order to better understand the obtained impedance responses for the duplex coating, the equivalent circuits that simulate the curves were developed (Figure **11**). For all cases, the model simulates the experimental data well, considering that the errors of fitting are lower than 5 % for all the parameters (Table **4**). After 5 min of immersion, the impedance response presents three capacitive semicircles which are simulated with three R//CPE sub-circuits. The Rs correspond to the solution resistance, the Rox//CPE1 element combination represents the oxides formed onto the steel surface, the R_{CT}//CPE2 is associated with the corrosion process where R_{CT} is the charge transfer resistance. Finally, the Rsf//CPE3 sub-circuit corresponds to the corrosion product layer [33]. As it was mentioned before, for 3 and 15 days, the impedance response differs in the low-frequency region in comparison to the response for 5 min. Instead of three R//CPE sub-circuits, these Nyquist curves were fitted with two R//CPE sub-circuits followed by a Warburg element, since a straight line of approximately 45° appears in the spectra [34]. This response is attributed to a corrosion process controlled by mass transfer limitations. The circuit described in Figure **11B** was already reported for duplex film onto Mg substrate

Table 4: Values for the Parameters of the Equivalent Circuit Obtained from the Best Fit to the Impedance Data

Parameter	5 min	3 days	15 days
Rs/ Ω cm^2	35	23.2	60.0
Rox/ Ω cm^2	103.4	108.4	36.6
R_{CT}/ Ω cm^2	232.5	174.8	193.1
Rsf/ Ω cm^2	4889.6	-	-
W*	-	1432.2	1354.5
P1/ F cm^{-2}	$1.35x10^{-4}$	$5.33x10^{-5}$	$3.00x10^{-7}$
n1	0.34	0.36	0.91
P2/ F cm^{-2}	$1.96x10^{-4}$	$3.81x10^{-5}$	$9.06x10^{-5}$
n2	0.42	0.77	0.64
P3/F cm^{-2}	$7.25x10^{-6}$	-	-
n3	1	-	-

[35]. According to the authors, the Rox//CPE1 circuit is associated with the polymer top layer whereas the values of Rct and W are related to the internal area of the duplex film.

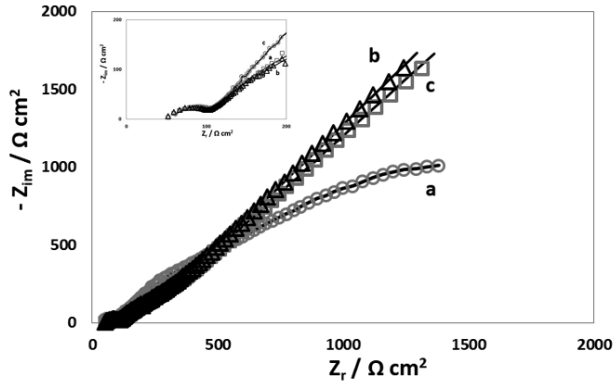

Figure 10: Nyquist plots of the impedance spectra for the Ce/PPy duplex coating at the open circuit potential in 0.50 M NaCl after different immersion time: 5 min (**a**), 3 days (**b**) and 15 days (**c**). (**d**) experimental data; (-) fitted data.

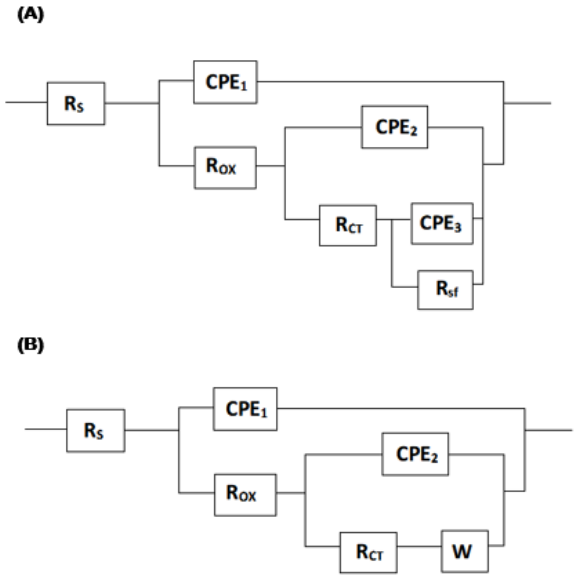

Figure 11: Equivalent circuit used for fitting experimental EIS data for Ce/PPy duplex coating: (**A**) at 5 min of immersion in 0.50 M NaCl and (**B**) 3 and 15 days of immersion in 0.50 M NaCl.

The R_{CT} is the main parameter for comparing the corrosion resistance of the coated substrate in different immersion times. As it could be seen from Table **4**, the R_{CT} the value for the film after 5 min is 232.5 Ω cm^2 and diminish after 3 days of immersion to 174.8 Ω cm^2, denoting that the duplex coating is losing its protective capacity. Finally, after 15 days of immersion, the R_{CT} value increases with respect to that corresponding to 3 days, being 193.1 Ω cm^2, this could be associated with an increment in the protective properties of the film due to the formation of a passive layer onto the substrate surface.

According to the results obtained here, it can be concluded that the superior anticorrosive properties obtained by Ce/PPy coating are due to the combination of the characteristics of each individual layer. Indeed, the cerium and chromium oxides in the inner layer act not only as a physical barrier but also provide a corrosion inhibition effect. In addition, the presence of AOT as an immobilized dopant in the outer polymeric layer due to its large size also contributes to the superior anticorrosive performance of the duplex coating. Moreover, PPy film on top of the cerium-based film reduces the film porosity and increases the barrier properties of the single film.

4. CONCLUSIONS

Double-layered cerium polypyrrole coating was obtained by a potentiostatic technique on AISI 304 SS. The adherent cerium layer was electrodeposited on steel as inner film. The outermost layer was a PPy film electrosynthesized in the presence of AOT. Ce film, PPy film and Ce/PPy coating all reduce the corrosion rate of the substrate in chloride solution. Specifically, the presence of the Ce/PPy film reduced the corrosion rate from 1.65 μA cm^{-2} to 0.06 μA cm^{-2}. Moreover, the Ce/PPy duplex coating showed improved anticorrosive performance compared to the single films. The quantity of Fe released was 2.60 and 2.10 mg/L for the substrate coated with Ce and PPy films and diminished to 1.44 mg/L when the alloy was covered with the duplex film. The enhancement of the corrosion resistance is associated with the combination of the characteristics of the single layers. In this way, the inner layer acts both as an adherence promoter for PPy film and as a corrosion inhibitor due to the presence of cerium and chromium oxides/hydroxides in the film. On the other hand, due to its large size, AOT remains entrapped into the polymer matrix as an immobilized dopant, which creates difficulties in the ingress of chloride ions through the coating. In addition, the polymeric outer layer seals the cerium film pores enhancing the physical barrier properties of the duplex coating.

ACKNOWLEDGEMENT

CONICET (PIP-112-201101-00055), ANPCYT (PICT-2015-0726) and Universidad Nacional del Sur (PGI 24/M159), Bahía Blanca, Argentina.

DECLARATIONS

Funding

CONICET (PIP-112-201101-00055), ANPCYT (PICT-2015-0726) and Universidad Nacional del Sur (PGI 24/M159), Bahía Blanca, Argentina.

Conflicts of Interest

The authors declare no conflicts of interest.

REFERENCES

[1] Sandu AV, Coddet C, Bejinariu C. A Comparative Study on Surface Structure of Thin Zinc Phosphates Layers Obtained Using Different Deposition Procedures on Steel. Rev. Chim. 2012; 63(4): 404-406.

[2] Ramezanzadeh B, Attar MM. Cathodic Delamination and Anticorrosion Performance of an Epoxy Coating Containing Nano/Micro-Sized ZnO Particles on Cr(III)-Co(II)/Cr(III)-Ni(II) Posttreated Steel Samples. Corrosion. 2013; 69(8): 793-803 https://doi.org/10.5006/0841

[3] Neri W. Introduzione alla Verniciatura delle superfici metalliche. 3rd ed. Tecniche Nuove. Milan (1990).

[4] Xingwen Y, Chunan C, Zhiming Y, Derui Z, Zhongda Y. Study of double layer rare earth metal conversion coating on aluminum alloy LY12. Corros. Sci. 2011; 43(7): 1283-1294. https://doi.org/10.1016/S0010-938X(00)00141-4

[5] Maddela S, O'Keefe MJ, Yang YM, Kuo HH. Influence of Surface Pretreatment on Coating Morphology and Corrosion Performance of Cerium Based Conversion Coatings on AZ91D Alloy. Corrosion. 2010; 66(11): 115006, 1-8. https://doi.org/10.5006/1.3516220

[6] Pepe A, Aparicio M, Durán A, Ceré S. Cerium hybrid silica coatings on stainless steel AISI 304 substrate. J Sol-Gel Sci Technol. 2006; 39(2): 131-138. https://doi.org/10.1007/s10971-006-9173-1

[7] Aggoun K, Chaal L, Creus J, Sabot R, Saidani B, Jeannin M. Marine corrosion resistance of CeO2/Mg(OH)2 mixed coating on a low alloyed steel. Surf. Coat. Technol. 2019; 372: 410-421. https://doi.org/10.1016/j.surfcoat.2019.05.053

[8] Qi Wang A, Golden T. Electrodeposition of Oriented Cerium Oxide Films. Int. Jour. Electrochem. (2013). https://doi.org/10.1155/2013/482187

[9] Ding K, Jia H, Wei S, Guo Z. Electrocatalysis of Sandwich-Structured Pd/Polypyrrole/Pd Composites toward Formic Acid Oxidation. Ind. Eng. Chem. Res. 2011; 50(11): 7077-7082. https://doi.org/10.1021/ie102392n

[10] Grgur BN, Krstaji NV, Vojnovi MV, Lanjevac C, Gaji-Krstaji Lj. The influence of polypyrrole films on the corrosion behavior of iron in acid sulfate solutions. Prog. Org. Coat. 1998; 33(1): 1-6. https://doi.org/10.1016/S0300-9440(97)00112-4

[11] Paliwoda-Porebska G, Stratmann M, Rohwerder M, Potje-Kamloth K, Lu Y, Pich A, Adler H. On the development of polypyrrole coatings with self-healing properties for iron corrosion protection. Corros. Sci. 2005; 47(12): 3216-3233. https://doi.org/10.1016/j.corsci.2005.05.057

[12] Herrasti P, Recio FJ, Ocon P, Fatas E. Effect of the polymer layers and bilayers on the corrosion behaviour of mild steel: Comparison with polymers containing Zn microparticles. Prog. Org. Coat 2005; 54(4): 285-291. https://doi.org/10.1016/j.porgcoat.2005.07.001

[13] Koene L, Hamer WJ, de Wit JHW. Electrochemical behaviour of poly(pyrrole) coatings on steel. J. Appl. Electrochem. 2006; 36(5): 545-556. https://doi.org/10.1007/s10800-005-9104-9

[14] Hosseini MG, Sabouri M, Shahrabi T (2007) Corrosion protection of mild steel by polypyrrole phosphate composite coating. Prog. Org. Coat. 2007; 60(3): 178-185. https://doi.org/10.1016/j.porgcoat.2007.07.029

[15] Zhang T, Zeng CL. Corrosion protection of 1Cr18Ni9Ti stainless steel by polypyrrole coatings in HCl aqueous solution. Electrochim Acta 2005; 50(24): 4721-4727. https://doi.org/10.1016/j.electacta.2005.01.049

[16] Blanco MX, Blanco Pinzon CE, García Vegara SJ. Synthesis and characterization of polypyrrole - TiO2 coatings on AISI 304 stainless Steel. J. Phys.: Conf. Ser. 2018; 1119: 1-6. https://doi.org/10.1088/1742-6596/1119/1/012029

[17] Jang L, Ma H, Zhang J, Lu Y, Lu H, Meng X. Electro Polymerization of Polypyrrole Coatings Doped with Different Proton Acids for Corrosion Protection of 304 Stainless Steel. MATEC Web Conferences. (2017). https://doi.org/10.1051/matecconf/201710903007

[18] El Jaouhari A, Chennah A, Ben Jaddi S, Ait Ahsaine H, Anfar Z, Tahiri Alaoui Y, Naciri Y, Benlhachemi A, Bazzaoui M. Electrosynthesis of zinc phosphate-polypyrrole coatings for improved corrosion resistance of steel. Surf. Interfaces. 2019; 15: 224-231. https://doi.org/10.1016/j.surfin.2019.02.011

[19] Omastová M, Trchová M, Pionteck J, Prokes J, Stejskal J. Effect of polymerization conditions on the properties of polypyrrole prepared in the presence of sodium bis(2-ethylhexyl) sulfosuccinate. Synth. Met. 2004; 143: 153-161 https://doi.org/10.1016/j.synthmet.2003.11.005

[20] Lehr IL, Saidman SB. Electrodeposition of polypyrrole on aluminium in the presence of sodium bis(2-ethylhexyl) sulfosuccinate. Mater. Chem. Phys. 2006; 100: 262-267. https://doi.org/10.1016/j.matchemphys.2005.12.041

[21] Lehr IL, Saidman SB. Corrosion protection of iron by polypyrrole coatings electrosynthesised from a surfactant solution. Corros. Sci. 2007; 49: 2210-2225 https://doi.org/10.1016/j.corsci.2006.10.033

[22] Flamini DO, Saidman SB. Characterization of polypyrrole films electrosynthesized onto titanium in the presence of sodium bis(2-ethylhexyl) sulfosuccinate (AOT). Electrochim. Acta. 2010; 55: 3727-3733. https://doi.org/10.1016/j.electacta.2010.01.107

[23] Johansen H, Brett C, Motheo A. Corrosion protection of aluminium alloy by cerium conversion and conducting polymer duplex coatings. Corros. Sci. 2012; 63: 342-350. https://doi.org/10.1016/j.corsci.2012.06.020

[24] Lavigne O, Alemany-Dumont C, Normand B, Delichére P, Descamps A. Cerium insertion in 316L passive film: Effect on conductivity and corrosion resistance performances of metallic bipolar plates for PEM fuel cell application. Surf. Coat. Techonol. 2010; 205(7): 1870-1877. https://doi.org/10.1016/j.surfcoat.2010.08.051

[25] Zhitomirsky I. Cathodic electrodeposition of ceramic and organoceramic materials. Fundamental aspects. Adv. Colloid Interface Sci. 2002; 97: 279-317. https://doi.org/10.1016/S0001-8686(01)00068-9

[26] Aldykiewicz Jr AJ, Davenport AJ, Isaacs HS. Studies of the Formation of Cerium-Rich Protective Films Using X-Ray Absorption Near-Edge Spectroscopy and Rotating Disk Electrode Methods. J. Electrochem. Soc. 1996; 143(1): 147-154. https://doi.org/10.1149/1.1836400

[27] Vakili R, Ramezanzadeh B, Amini R. The corrosión performance and adhesión properties of the epoxy coating applied on the steel substrates treated by cerium-based conversión coating. Corros. Sci. 2015; 94: 466-475. https://doi.org/10.1016/j.corsci.2015.02.028

[28] Ocón P, Cristobal A, Herrasti P, Fatas E. Corrosion performance of conducting polymer coatings applied on mild steel. Corros. Sci. 2005; 47: 649-662. https://doi.org/10.1016/j.corsci.2004.07.005

[29] Fenelon A, Breslin C. Polyaniline-coated iron: studies on the dissolution and electrochemical activity as a function of pH. Surf. Coat. Technol. 2005; 190: 264-270 https://doi.org/10.1016/j.surfcoat.2004.04.083

[30] Lei L, Shi J, Wang X, Liu D, Xu H. Microstructure and electrochemical behavior of cerium conversion coating modified with silane agent on magnesium substrates. Appl. Surf. Sci. 2016; 376: 161-171. https://doi.org/10.1016/j.apsusc.2016.03.150

[31] Tomic M, Petrovic M, Stankovic S, Stevanovic S, Bajat JB. Ternary Zn-Ni-Co alloy: anomalous codeposition and corrosion stability. J. Serb. Chem, Soc. 2015; 80(1): 73-86 https://doi.org/10.2298/JSC260814113B

[32] Bajat JB, Vasilic R, Stojadinovic S, Miskovic-Stankovic V. Corrosion stability of oxide coating forme by plasma electrolytix oxidation of aluminum optimization of process time. Corrosion. 2013; 69(7): 693-702. https://doi.org/10.5006/0859

[33] G. Cai, H. Wang, D. Jiang, Z. Dong, Degradation of fluorinated polyurethane coating under UVA and salt spray. Part I: Corrosion resistance and morphology, Prog. Org. Coatings. 2018; 123: 337-349. https://doi.org/10.1016/j.porgcoat.2018.07.025

[34] X. Huang, N. Li, H. Wang, H. Sun, S. Sun, J. Zheng, Electrodeposited cerium film as chromate replacement for tinplate, Thin Solid Films. 2008; 516: 1037-1043. https://doi.org/10.1016/j.tsf.2007.08.044

[35] M. Toorani, M. Aliofkhazraei, Review of electrochemical properties of hybrid coating systems on Mg with plasma electrolytic oxidation process as pretreatment, Surfaces and Interfaces. 2019; 14: 262-295. https://doi.org/10.1016/j.surfin.2019.01.004

Received on 20-04-2021 Accepted on 01-06-2021 Published on 24-06-2021

DOI: https://doi.org/10.15377/2410-4701.2021.08.1